Diastereomer-Specific Effects of Double-Stranded Peptides Conjugated with –L-Tyr–L-Phe– or –L-Tyr–D-Phe– Residues on Tyrosine Phosphorylation and Inhibition of *src*^{ts}NRK, A431, MCF-7, and DU145 Cell Growth

Shigeki KOBAYASHI,*[,a] Nahomi ATUCHI,[a] Hidetaka WAKAMATSU,[a] Mayuko HATTORI,[a] Ayumi KAWADA,[a] and Kouji ASANO[b]

[a] *Division of Analytical Chemistry of Medicines, Showa Pharmaceutical University; 3–3165 Higashi-tamagawagakuen, Machida, Tokyo 194–8543, Japan: and* [b] *Department of Urology, Jikei University School of Medicine; 3–25–8 Nishi-shinbashi, Minato-ku, Tokyo 105–8461, Japan.* Received June 6, 2007; accepted September 1, 2007

The interaction between growth inhibition and chirality, especially of diastereomers, has an important modifying effect on cancer cell proliferation. Previously, we have reported on the design, synthesis, and chemical properties of a series of novel, double-stranded peptides, (y-AA–x-AA)$_2$-(CH$_2$)$_{12}$, with –y-AA–x-AA– and –z-AA–y-AA–x-AA– sequences conjugated to the spacer. Here, we extend those results by showing that (D-, L-) and (L-, D-) diastereomers are more potent inhibitors of tyrosine phosphorylation than (L-, L-). Although the replacement of the L-Phe–L-Phe sequence with L-Tyr–L-Phe produces a less active inhibitor, the double-stranded peptide conjugated with L-Tyr–D-Phe is more active than that conjugated with L-Tyr–L-Phe. In addition, we show that SDS-PAGE gel profiles of tyrosine phosphorylation following treatment with bis(y-Tyr–x-Phe)-*N*,*N*-dodecane-1,12-diamine appear very similar to profiles of tyrosine phosphorylation following treatment with an analog of the tyrosine kinase inhibitor, erbstatin. Moreover, the level of autophosphorylation of the epidermal growth factor receptor kinase domain (EGFRKD) treated with bis(L-Tyr–D-Phe)-*N*,*N*-dodecane-1,12-diamine was lower than that seen following treatment with bis(L-Phe–D-Phe)-*N*,*N*-dodecane-1,12-diamine. These data provide new insights for the control of cancer cell proliferation through drug designs which replace the less active –L-Phe–L-Phe– (and –D-Phe–L-Phe–) with the more active –L-Tyr–L-Phe- (and –L-Tyr–D-Phe–) sequence.

Key words double-stranded peptide; chirality; cell growth inhibition; diastereomer; tyrosine phosphorylation; epidermal growth factor receptor kinase domain

Signal transduction factors that mediate cell division and growth such as protein tyrosine and serine kinases play important roles in many proliferative diseases. Binding of ligands to specific cell-surface receptors leads to aberrant signals, such as gene deletion and abnormal protein function, which lead to abnormal proliferation.[1,2] Better understanding these pathways can potentially aid in designing drugs that inhibit malignant neoplastic proliferation. Tyrosine (Tyr), with its phenol side chain, provides a phosphorylation site for tyrosine kinases, which play an important role in signal transduction (such as SH2 and SH3 domains).[3] From a pharmacological viewpoint, drugs which contain Tyr residues in their structure compete for tyrosine kinase phosphorylation and may affect the signal transduction of living cells.

Recently, we reported the relationship between optical isomers and growth inhibition activity by using a set of parallel, double-stranded peptides, bis(y-Phe–x-Phe)$_2$–spacer(S) (**7**) (symbols x and y=L- or D-configurations, AA=amino acid, and S=(CH$_2$)$_{12}$, with two Phe residues conjugated to a polyamine spacer as a model of neoplastic targeting.[4—6] In order to elucidate the relationship between chirality and effect of Tyr on cell growth inhibition by the double-stranded peptides, we synthesized the bis(y-Tyr–x-Phe)$_2$–(CH$_2$)$_{12}$ (**6**) replacing y-Phe–x-Phe with y-Tyr–x-Phe sequence. To elucidate the mechanism of action of the compound, we assayed (i) the change in the level of tyrosine phosphorylation of total proteins of *src*^{ts}NRK cells, and (ii) the inhibition of epidermal growth factor receptor protein tyrosine kinase domain (EGFRKD) autophosphorylation [7,8] following treatment with **6** or **7**. The proliferation of these cells is regulated by tyrosine phosphorylation and dephosphorylation, by tyrosine kinases and tyrosine phosphatases, respectively.

The results showed that bis(L-Tyr–L-Phe)-*N*,*N*-dodecane-1,12-diamine (**6a**) and bis(L-Tyr–L-Ile)-*N*,*N*-dodecane-1,12-diamine (**6e**), containing the L-Tyr–L-Phe and L-Tyr–L-Ile sequences, markedly increased the tyrosine phosphorylation of 32—34 kDa proteins in *src*^{ts}NRK cells. However, the profiles of the total phosphotyrosine of proteins from cells treated with **7a** and **7b**, containing L-Phe–L-Phe and D-Phe–L-Phe sequences, are strikingly different from the profiles of those treated with **6a** and **6e**. The action of **6a** on the tyrosine phosphorylation of proteins in *src*^{ts}NRK cells is very similar to that of the tyrosine kinase inhibitor, erbstatin.[9] The EGF-R protein tyrosine kinase, a transmembrane glycoprotein, is one target for the treatment of proliferative diseases.[8,10] Our results show that compounds **6a** and **6b** are inhibitors of EGF-R tyrosine phosphorylation.

Thus, we believe that the double-stranded peptides, **6a**, **b** and **6c**, **d**, can be used to control the inhibitory effect on proliferation shown by both diastereomers, (D-, L-) and (L-, D-), and we describe new insights which could explain the different inhibitory effects on proliferation of Phe and Tyr, (D-, L-) and (L-, L-) forms.

Experimental

General Synthetic Methods The general synthetic approach for all compounds is described elsewhere.[4,5] The peptides were detected on TLC plates using iodine vapor or UV absorption. Silica gel column chromatography was performed on Silica gel 60N (100 mesh, neutral, Kanto Chemical Co.). Solvent systems were as follows, A: $CHCl_3$–MeOH (20 : 1), and B: $CHCl_3$–MeOH (10 : 1). Analytical reverse-phase HPLC was carried out

* To whom correspondence should be addressed. e-mail: kobayasi@ac.shoyaku.ac.jp

using a TOSO CCPD system equipped with a Tskgel (ODS-120T) column. Infrared (IR) spectra were recorded with a JASCO A100 spectrometer. The pH was measured by TOA pH instrument (Model HM-7E). ^{1}H- and ^{13}C-NMR spectra were obtained using a JEOL α-500 or GX270 NMR spectrometers and NMR samples were dissolved in DMSO-d_6/$CDCl_3$ (ratio: 0.5 ml/0.2 ml) with TMS as an internal reference. FAB mass spectral data were obtained on a JEOL JMS-HX110 spectrometer, and relevant data were tabulated as *m/z*. Elemental analyses were performed by the Laboratory Center of Elemental Analysis, University of Ehime (Ehime, Japan).

Synthesis of Bis(peptides)-*N*,*N*-dodecane-1,12-diamine The double-stranded peptides, **6a**—**e** and **7a**, **b** used in this study were prepared according to the procedures described in our previous papers.[4,5]

Bis(L-Tyr(OBzl))-*N*,*N*-dodecane-1,12-diamine (3c) Boc–L-Tyr(OBzl)OH (3.13 g, 8.44 mmol) and CDI (1.64 g, 10.12 mmol) were dissolved in dry $CHCl_3$ (35 ml). The mixture was stirred for 1.0 h, and to this was added 1,12-diaminododecane (0.82 g, 4.1 mmol) at 4 °C. The solution was stirred overnight. The solvent was evaporated to dryness. After the addition of aqueous MeOH, the precipitate was collected, washed with 5% citric acid, 5% $NaHCO_3$, and aqueous MeOH, and dried *in vacuo*. The resulting crude product, bis(Boc–L-Tyr(OBzl))-*N*,*N*-dodecane-1,12-diamide (**2c**), a colorless solid, was obtained in 94.0% yield. The crude product (3.5 g) was purified by chromatography on silica gel column (40 g) and eluted in $CHCl_3$ and 2% MeOH/$CHCl_3$ (stepwise elution); mp 194—196 °C (from MeCN); *Rf* (A): 0.87. HR-FAB-MS (nitrobenzylalchohol, NBA) Calcd for $C_{54}H_{75}N_4O_8$ ($M+H^+$) *m/z*: 907.5587. Found: 907.5571.

To compound **2c** (4.57 g, 5.04 mmol) was added TFA (26 ml). The mixture was stirred for 1 h in an ice bath. After a 5% $NaHCO_3$ and 1 mol/l NaOH workup and the mixture was stored at ice bath, solid **3c** was collected, washed with water, dried *in vacuo*, and was obtained in 72.1% yield. Compound **3c** was purified by silica gel column chromatography eluted with $CHCl_3$, 3% MeOH/$CHCl_3$ (stepwise elution); mp 144—146 °C (from MeCN); *Rf* (B): 0.45. ^{1}H-NMR ($CDCl_3$/DMSO-d_6=0.5/0.2 ml) δ 1.20—1.28 (m, 8H, –(CH_2)– ×4), 1.42—1.50 (m, 2H, –(CH_2)– in spacer), 2.66 (dd, *J*=8.25, 13.73 Hz, 1H, βH in Tyr), 3.04 (dd, *J*=4.57, 13.73 Hz, 1H, βH in Tyr), 3.12—3.18 (m, 2H, –CH_2NHCO– in spacer), 3.47 (dd *J*=4.57, 8.25 Hz, 1H, αH in Tyr), 5.04 (s, 2H, –O–CH_2–C_6H_5), 6.89 (d, *J*=8.55 Hz, 2H, Tyr), 7.13 (d, *J*=8.55 Hz, 2H, Tyr), 7.29—7.42 (m, 5H, benzyl), and 7.49 (t, *J*=5.90 Hz, 1H, –NH^aCO–); ^{13}C-NMR ($CDCl_3$/DMSO-d_6=0.5/0.2 ml) ppm 26.72, 29.08, 29.31, 29.33, 38.83, 40.21, 56.30, 69.69, 114.68, 127.34, 127.77, 128.39, 130.22, 130.34, 136.97, 157.31, and 174.17. FAB-HR-MS (NBA) Calcd for $C_{44}H_{59}N_4O_4$ ($M+H^+$) *m/z*: 706.4530: Found 707.4552.

Bis(L-Tyr–L-Phe)-*N*,*N*-dodecane-1,12-diamine (6a) CDI (1.66 g, 10.2 mmol) was added to a solution of Boc–L-Tyr(OBzl)OH (3.16 g, 8.53 mmol) in dry $CHCl_3$ (35 ml). After stirring for 1.0 h at room temperature, compound (**3a**)[4] (2.0 g, 4.06 mmol) was added, then the solution was stirred overnight. Compound bis(Boc–L-Tyr(OBzl)–L-Phe)-*N*,*N*-dodecane-1,12-diamide (**4a**), a colorless solid, was prepared in a similar manner to that for **2c** and obtained in 97.0% yield. The crude product (4.5 g) was purified by chromatography on silica gel column (43 g) and eluted in $CHCl_3$ and 3% MeOH/$CHCl_3$ (stepwise elution); mp 199—200 °C (from MeOH); *Rf* (A): 0.65; FAB-MS (nitrobenzyl alcohol) *m/z* 1022 $(M+H)^+$. To a solution of **4a** (2.50 g, 2.08 mmol) in methanol (100 ml) was added 5% Pd/C (0.50 g). The mixture was shaken under H_2. After the reaction was completed, the catalyst (**5a**) was removed by filtration and obtained in 86.0% yield. Compound **5a** was purified by silica gel column chromatography and eluted with $CHCl_3$ and 3% MeOH/$CHCl_3$ (stepwise elution); mp 132—135 °C (from MeOH); *Rf* (B): 0.46. *Anal.* Calcd for $C_{58}H_{80}N_6O_{10}\cdot 1/2H_2O$; C, 67.61; H, 7.92; N, 8.16. Found: C, 67.66; H, 7.94; N, 8.25.

Compound **5a** (2.0 g, 2.39 mmol) was dissolved in TFA (15 ml). The colorless solid **6a** was collected in a similar manner to that for **3c**. Compound **6a** was purified by silica gel column chromatography eluted with $CHCl_3$, 3% MeOH/$CHCl_3$, and 8% MeOH/$CHCl_3$ (stepwise elution); mp 178—180 °C (from MeCN/MeOH); *Rf* (B): 0.10; IR (KBr) cm^{-1} 3296 (m), 2920 (m), 1648 (s); ^{1}H-NMR ($CDCl_3$/DMSO-d_6=0.5/0.2 ml) δ 1.15—1.24 (m, 8H, –(CH_2)– ×4), 1.36—1.39 (m, 2H, –(CH_2)– in spacer), 2.45 (dd, *J*=8.85, 13.73 Hz, 1H, βH^1 in Phe^1), 2.89 (dd, *J*=4.27, 13.73 Hz, 1H, βH^2 in Tyr^2), 2.93 (dd, *J*=7.63, 13.74 Hz, 1H, βH^1 in Phe^1), 3.00—3.18 (m, 3H, βH^2 in Tyr^2 and –CH_2NHCO–), 3.49 (dd, *J*=4.27, 8.85 Hz, 1H, αH^2 in Tyr^2), 4.62 (ddd, *J*=7.63, 8.55, 8.85 Hz, 1H, αH^1 in Phe^1), 6.72 (d, *J*=8.55 Hz, 2H, Tyr^2), 6.96 (d, *J*=8.54 Hz, 2H, Tyr), 7.14—7.19 (m, 3H, Phe^1), 7.22—7.26 (m, 2H, Phe^1), 7.44 (t, *J*=5.49 Hz, 1H , –NH^aCO–), and 7.98 (d, *J*=8.55 Hz, 1H, –NH^bCO–); ^{13}C-NMR ($CDCl_3$/DMSO-d_6=0.5/0.2 ml) ppm 26.65, 29.05, 29.15, 29.28, 29.30, 38.38, 39.09, 39.72, 53.64, 56.18, 115.39, 126.38, 127.73, 128.06, 129.31, 130.08, 137.14, 156.08, 170.63 and 173.67. *Anal.* Calcd for $C_{48}H_{64}N_6O_6\cdot 1/2H_2O$: C, 69.45; H, 7.89; N, 10.12. Found: C, 69.11; H, 7.84; N, 9.99.

Spectral Data for Bis(L-Tyr–D-Phe)-*N*,*N*-dodecane-1,12-diamine (6b) Compound **6b** was prepared in a similar manner to **6a** and obtained as a colorless solid in 69.0% yield; mp 135—137 °C; from (ether/MeOH), *Rf* (B): 0.08; IR (KBr) cm^{-1} 3300 (m), 2920 (m), 1650 (s); ^{1}H-NMR ($CDCl_3$/DMSO-d_6=0.5/0.2 ml, α-500) δ 1.20—1.25 (m, 8H, –(CH_2)– ×4), 1.39—1.42 (m, 2H, –(CH_2)–), 2.59 (dd, *J*=7.63, 14.03 Hz, 1H, βH^1 in Tyr^2), 2.81 (dd, *J*=5.50, 14.03 Hz, 1H, βH^2 in Tyr^2), 2.83 (dd, *J*=8.24, 13.43 Hz, 1H, βH^2 in Phe^1). 3.09—3.24 (m, 3H, –CH_2NHCO– and βH^1 in Phe^1), 4.01 (dd, *J*=5.50, 7.63 Hz, 1H, αH^2 in Tyr^2), 4.59 (ddd, *J*=4.88, 8.24, 8.54 Hz, 1H, αH^1 in Phe^1), 6.67 (d, *J*=8.55 Hz, 2H, Tyr^2), 6.81 (d, *J*=8.24 Hz, 2H, Tyr), 7.15—7.26 (m, 5H, Phe^1), 7.81 (t, *J*=5.50 Hz, 1H, –NH^aCO–), and 8.73 (d, *J*=8.54 Hz, 1H, –NH^bCO–); ^{13}C-NMR ($CDCl_3$/DMSO-d_6=0.5/0.2 ml) ppm 26.67, 29.05, 29.20, 29.26, 29.28, 38.37, 38.09, 39.22, 54.31, 54.81, 115.55, 124.77, 126.46, 128.13, 129.31, 130.46, 137.55, 156.67, 168.39, and 170.54. FAB-HR-MS (NBA) Calcd for $C_{48}H_{65}N_6O_6$ ($M+H^+$) *m/z*: 821.4967. Found: 821.4958.

Spectral Data for Bis(L-Phe–L-Tyr-*N*,*N*-dodecane-1,12-diamine (6c) Compound **6c** was prepared in a similar manner to **6a** and obtained as a colorless solid in 75.0% yield; mp 181—184 °C; from (ether/MeOH), *Rf* (B): 0.11; IR (KBr) cm^{-1} 3309 (m), 2853 (m), 1648 (s), 1628 (s); ^{1}H-NMR ($CDCl_3$/DMSO-d_6=0.5/0.2 ml, α-500) δ 1.20—1.28 (m, 8H, –(CH_2)– ×4), 1.37—1.43 (m, 1H, –(CH_2)–), 2.70 (dd, *J*=8.55, 13.73 Hz, 1H, βH^2), 2.83 (dd, *J*=7.93, 13.73 Hz, 1H, βH^1), 2.92 (dd, *J*=5.80, 13.74 Hz, 1H, βH^1), 3.05—3.12 (m, 3H, –CH_2NHCO– and βH^2), 3.70 (dd, *J*=4.88, 8.55 Hz, 1H, αH^2), 4.53 (ddd, *J*=6.41, 7.93, 8.55 Hz, 1H, αH^1), 6.69 (d, *J*=8.55 Hz, 2H, Tyr), 6.97 (d, *J*=8.55 Hz, 2H, Tyr), 7.19—7.21 (m, 2H, Phe), 7.22—7.46 (m, 3H, Phe), 7.46 (t, *J*=5.50 Hz, 1H, –NH^aCO–), and 8.19 (d, *J*=8.55 Hz, 1H, –NH^bCO–); ^{13}C-NMR ($CDCl_3$/DMSO-d_6=0.5/0.2 ml) ppm 26.66, 29.03, 29.18, 29.26, 29.28, 37.53, 39.06, 39.43, 54.38, 55.42, 115.13, 126.63, 127.41, 128.37, 129.32, 130.17, 136.90, 155.99, 170.73, and 171.84. FAB-HR-MS (NBA) Calcd for $C_{48}H_{65}N_6O_6$ ($M+H^+$) *m/z*: 821.4965. Found: 821.4971.

Spectral Data for Bis(L-Tyr–L-Ile)-*N*,*N*-dodecane-1,12-diamine (6e) Compound **5e** (81.5% yield) prepared in a similar manner to **5a** was purified by silica gel column chromatography, eluted with $CHCl_3$ and 3% MeOH/$CHCl_3$ (stepwise elution); mp 199—201 °C (from MeOH); *Rf* (B): 0.49. *Anal.* Calcd for $C_{52}H_{84}N_6O_{10}$: C, 65.51; H, 8.88; N, 8.82. Found: C, 65.21; H, 9.00; N, 8.72. Compound **6e** was prepared in a similar manner to **6a** and obtained as a colorless solid in 83.0% yield: mp 190—193 °C (from MeCN/MeOH); *Rf* (B): 0.10; IR (KBr) cm^{-1} 3298 (m), 2931 (m), 1678 (s), 1643 (s); ^{1}H-NMR ($CDCl_3$): δ 0.85—0.89 (m, 6H, βMe and δMe, Ile), 1.07—1.15 (m, 1H, γH in Ile), 1.20—1.30 (m, 8H, –$(CH_2)_n$– in spacer), 1.44—1.50 (m, 3H, γH(Ile) and –CH_2–), 1.78—1.82 (m, 1H, βH in Ile), 2.92 (dd, *J*=7.63, 14.3 Hz, 1H, βH in Tyr), 3.08—3.19 (m, 3H, β proton in Tyr and –CH_2NHCO–), 4.11 (m, 1H, αH^2 in Tyr), 4.22 (m, 1H, αH^1 in Ile), 6.73 (d, *J*=8.2 Hz, 2H, Tyr), 7.05 (d, *J*=8.5 Hz, 2H, Tyr), 7.52 (t, *J*=5.50 Hz, 1H, –NH^aCO–), 8.56 (d, *J*=8.85 Hz,1H, –NH^bCO–); ^{13}C-NMR ($CDCl_3$/DMSO-d_6=0.5/0.2 ml) ppm 11.19, 15.37, 24.59, 26.71, 29.01, 29.21, 29.24, 29.28, 36.47, 37.02, 38.99, 54.12, 58.10, 115.59, 124.76, 130.49, 156.71, 168.14, and 170.55. FAB-HR-MS (NBA) Calcd for $C_{42}H_{69}N_6O_6$ ($M+H^+$) *m/z*: 753.5285. Found: 753.5260.

UV/Vis Titration The acid-base dissociation constant (pK_a) was obtained by the UV/Vis titration method. Compounds **6a** and **6e** were brought to a final concentration of 3.65×10^{-5} mol/l, the pH in the solution increased from 4.9 to 12.6 at 297 (K) as a function of pH in a 10-mm path length quartz cell. Various pH (pH=4.9, 6.1, 6.4, 7.7, 8.2, 8.8, 9.2, 10.4, 11.7, 12.2, 12,6) solutions were prepared with 0.1 mol/l acetate, 0.1 mol/l sodium acetate, 0.2 mol/l borate-sodium chloride, and 0.2 mol/l sodium hydroxide buffer in 85% MeOH solution.

Computational Chemistry The search for optimized conformations of double-stranded peptides were done using SPARTAN'04 programs[11] running on a personal computer (Pentium 4 CPU). The lowest energy conformer determined with the conformationanl search (Monte-Carlo method) computation at the MMFF94 level was optimized using the restricted Hartree-Fock (RHF) level with a 6-31G(d) basis set.

Drugs and Chemicals Dulbecco's Modified Eagle Medium (DMEM) and fetal bovine serum (FBS) were obtained from Dainippon Pharma Co., Ltd. (Tokyo). The cellular toxicity kit (WST-1 or Kit-8) was obtained from Dojindo Laboratories (Kumamoto, Japan). The small double-stranded modified peptides were synthesized according to previously published methods.[4,5] POD (peroxidase)-conjugated anti-phosphotyrosine monoclonal antibody (PY20, M141) was purchased from TAKARA Bio Inc., (Tokyo,

Japan). This antibody is specific for phosphotyrosine in proteins and does not cross-react with phosphoserine, phosphothreonine, or phosphohistidine, *etc*. Erbstatin analog (**8b**) was purchased from Wako Pure Chemical Ind., Ltd. (Osaka, Japan). All other chemicals were obtained from Sigma-Aldlich Inc. (St. Louis, MO, U.S.A.) and Wako Pure Chemical Ind., Ltd.

Cell Line and Culture The A431[12] and A549[13] cell lines were obtained from RIKAGAKU institute (Tukuba, Japan), and the *src*^{ts}NRK cell line was donated by Prof. K. Tsuchiya (Showa Pharmaceutical University, Tokyo).[14,15] Stock cells were cultured in DMEM containing 0.37% sodium bicarbonate, 100 units/ml of penicillin G, and 100 μg/ml streptomycin sulfonate supplemented with 10% heat inactivated FBS, in a water-jacketed 5% CO_2 incubator; the medium was exchanged every three to four days. For the experiments, the cells were seeded at a density of 5.0×10^5 cells/ml in tissue culture flasks (25 cm^2/ml) in 10% FBS/DMEM. Breast cancer MCF-7 cells were obtained from Human Science of Japan (Osaka) and grown in phenol red-free RPMI1640 medium (GIBCO, Life Technologies, Basel, Switzerland) containing 23.8 mM $NaHCO_3$ and supplemented with 5% fetal calf serum (FCS), penicillin G (10000 units/l), and streptomycin sulfonate (10 mg/l) (the medium).[16] MCF-7 cells were maintained in 75 cm^2 culture flasks and incubated in a humidified mixture of 5% CO_2 under atmospheric pressure at 37 °C.

Cell Growth Inhibition Assay To measure the effect on cell proliferation by various concentrations of the double-stranded and single stranded peptides, *src*^{ts}NRK cells ($1.0—2.0\times10^5$ cells/ml) were reseeded in flat bottom 96-well microtiter plates (180 μl/well) and incubated for 24 h at 33 °C (or 39 °C). The double-stranded peptides diluted in dimethylsulufoxide (DMSO) (5V/V%) were then added to the microtiter plates and incubated for 3 d at 33 °C (or 39 °C) in a humidified atmosphere containing 5% CO_2. Standard cell counting methods were used to assess cell growth. Cell viability was measured by WST-1 10 μl assay (or Kit-8), and the results were confirmed by scanning with a microplate reader (Model680, BIO-RAD, U.S.A.).

Cell Extracts Exponentially growing *src*^{ts}NRK cells were washed with PBS(−) and incubated in DMEM containing 5% FBS for 24 h at 37 °C in ten 75 cm^2 culture flasks. *Src*^{ts}NRK cells were incubated without (control) and with (experimental) **7a** (1.3×10^{-5} mol/l), **7b** (1.9×10^{-6} mol/l), **6a** (1.4×10^{-5} mol/l), **6e** (1.1×10^{-5} mol/l), and **8b** (8.8×10^{-6} mol/l) at 37 °C for 0.5 and 24.0 h, respectively. After treatment, cells (2.5×10^8 cells/ml) were washed with cold PBS(−) and lysed in lysis buffer (ISOGEN) at 4 °C for 15 to 20 min.

Gel Electrophoresis and Immunoblotting Cell lysate samples containing 100 μg of protein for SDS-PAGE on 10×10 cm gels (TECHNICAL FRONTIR CO., Tokyo), 1.5-mm thick, were mixed 1 : 1 with 5% SDS sample buffer containing 2-mercaptoethanol, and heated at 95 °C for 5 min prior to 8% SDS-PAGE gel electrophoresis. After electrophoresis, proteins were transferred to PVDF membrane in buffer containing 25 mmol/l Tris, 120 mmol/l glycine, and 2% MeOH at 180 mA for 3 h at 4 °C. The membrane was blocked by incubating in PBS(−) containing 2% ABS and 0.02% Tween 20 for 3 h at room temperature. The membranes were washed in 25 mmol/l Tris–HCl, 150 mmol/l NaCl, and 0.01% Tween 20, and incubated with POD-conjugated anti-phosphotyrosine monoclonal antibody (clone PY20; 9 μl/6 ml in 1% BSA-PBS(−)) at room temperature for 3 h. The conjugated antibody was removed, and the blotted membrane washed 3 times in the buffer. Proteins were detected using diaminobendizine (7.5 to 8.0 mg) in PBS(−) and 30% hydrogen peroxide (25 μl) under standard conditions. The amount of protein was analyzed by the Lowry method.

Autophosphorylation of EGFRKD Four microliters of double-stranded peptides (2.0×10^{-5} mol/l) solution were added to reaction buffer (50 mmol/l HEPES, 200 mmol/l Na_2VO_4, 40 mmol/l $MnCl_2$ and 1 mmol/l rATP, pH=7.4) containing 10 μl of EGFRKD (10 ng/ml; #206101, Stratagen, U.S.A.). The reaction was then diluted to a final volume of 40 μl. The mixture was incubated at 22 °C for 10 min. A 30 μl sample of the reaction mixture was analyzed by Western blotting using POD (peroxidase)-conjugated anti-phosphotyrosine monoclonal antibody, as described above.

Results and Discussion

Synthesis, Conformation, and Chemical Properties The double-stranded peptides used in this study were synthesized using procedures described in our previous papers.[4,5] Protected (*N*-^{t}Boc, *tert*-butoxycarbonyl) amino acids were coupled to a polyamine spacer to yield-protected, double-stranded peptides by the C-activating method using *N*,*N*-carbonyl diimidazole (CDI) in dry $CHCl_3$ (Fig. 1). The protected crude compound (**4a**) was purified using chromatography over silica gel 60 N (100 mesh, neutral). After purification, the benzyl protecting group of Tyr was removed with H_2 under 5% Pd–C in MeOH to yield compound **5a** (65%). After purification, the Boc protecting group was removed by treatment with trifluoroacetic acid (TFA) to produce bis(L-Tyr–L-Phe)-*N*,*N*-dodecane-1,12-diamine (**6a**) at 4 °C. The target compounds **6b**, **c**, **d** and **e** were prepared in a similar method as that for **6a** according to the synthetic route depicted in Fig. 1. The identity of all novel compounds was confirmed by TLC, ^{1}H- and ^{13}C-NMR, FAB-HR, and elemental analysis. The conformations of these compounds were determined from the dimensional (2D) C–H COSY and the intrastranded NOE assignment experiments.

In the 500 MHz ^{1}H-NMR spectrum in $CDCl_3$/DMSO-d_6 (0.5/0.2=0.7 ml), the chemical shifts of two amido protons, –NH^{a}CO– and –NH^{b}CO–, of compound **6a** were measured at 7.98 and 7.44 ppm, respectively. The spin coupling constant between amido proton (–NH^{a}CO–) and αH^a (Phe^a) was $^3J_{NH^a,\alpha H^a}$=8.5 Hz. The results suggest that compound **6a** adopts a β-sheet-like structure, because the coupling constant of 7.0—10.0 Hz is within the expected range for this structure.[4,17] The structure of –L-Tyr–D-Phe– in compound **6b** is also a β-sheet-like structure ($^3J_{NH^a,\alpha H^a}$=8.5 Hz). As the 3D-structure could not be determined from the NMR data, the conformation was investigated using computational chemistry and UV/Vis analysis.

Our aim was to determine the stereo-structure of peptides **6a** and **6b** containing a Tyr residue and compare these to those of **7a** and **7b**. In compound **6a** the two –L-Phe–L-Phe– strands in from compound **7a** are replaced with two –L-Tyr–L-Phe– strands. Using the HF method, results showed that the total energy (E_{total}) of **6a** and **6b** is larger than that of **7a** and **7b** at 6-31G(d) basis set label in the gas phase as listed in Table 1. Compounds **6b** and **7b** containing D-Phe have −6907545.88 and −6514454.98 kJ/mol lower total energy than **6a** and **7a**, respectively. In addition, these two compounds each have different conformations. In general, the conformation of double-stranded peptides is determined by (i) peptide sequences and (ii) species of the spacer. Table 1 shows the hydrophobicity ($\log P$) of –Phe–Phe– and –Tyr–Phe– sequences calculated with Ghose–Crippen method.[18] The $\log P$ of β-sheet like –Tyr–Phe– sequence is 1.797 smaller than that of the β-sheet like –Phe–Phe– sequence. It was found that compounds **6a** and **6b** are more hydrophilic than **7a** and **7b**. The optimized folding conformations of **6a** and **6b** are shown in Fig. 2.

According to the Bronsted–Lowry definition, the phenolic proton is a weak acid, as expressed in the following equilibrium:

$$C_6H_5OH \rightleftarrows C_6H_5O^- + H^+ \quad (1)$$

The pK_a value is 11.3 (9.89 in aqueous solution) in 85% MeOH solution. This suggests that the pK_a values of the double-stranded peptides **6a** and **6e** would be different from that of the phenolic proton. To better understand the chemical behavior of the phenolic proton of Tyr in double-stranded peptides, the pK_a value was measured using the UV/Vis titration method. The results are shown in Fig. 3 and Table 1.

The acid-base equilibrium of **6a**—**c** and **10** were studied

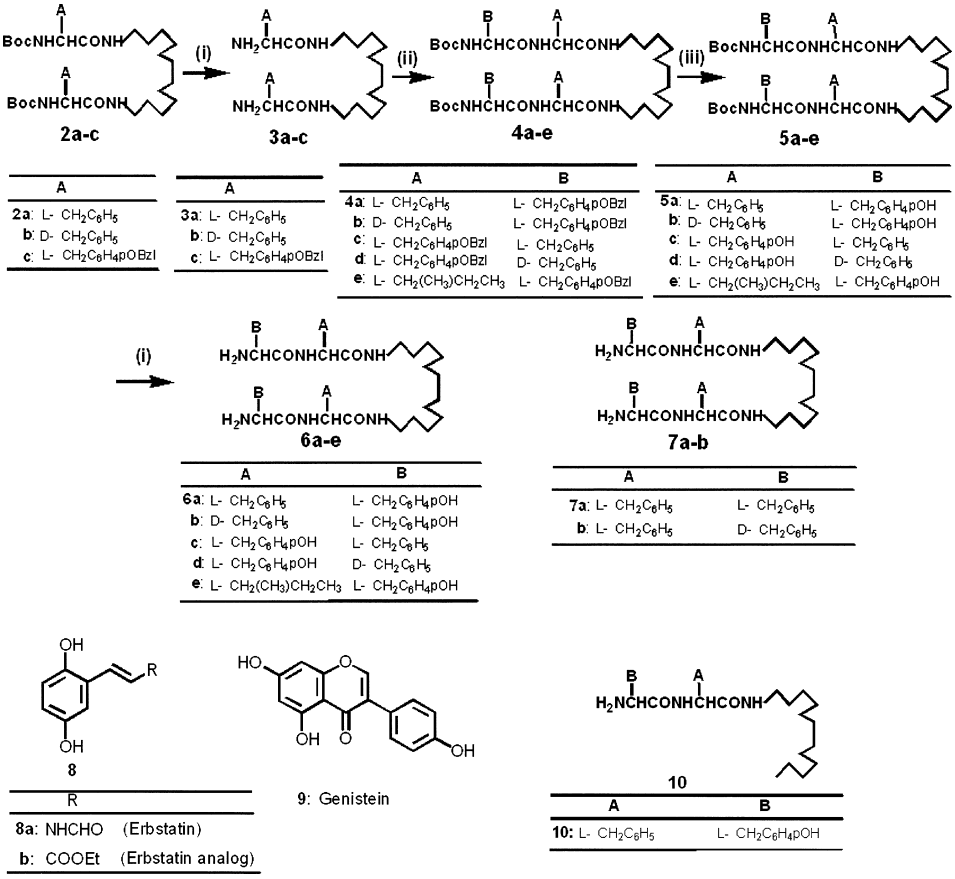

Fig. 1. Synthesis of Mini Parallel Double-Stranded Peptides Conjugated with –x-Phe–y-Phe– Sequences and Structures of Used Compounds in this Study

Key: (i) TFA at 4 °C; (ii) Boc–x-PheOH or Boc–x-Tyr(OBzl)OH (symbol x indicates L- or D-configuration), CDI, dry $CHCl_3$; (iii) 5% Pd–C/H_2, MeOH or DMF/MeOH.

Table 1. Difference of Chemical Properties between Phe–Tyr and Phe–Phe Resides in Double-Stranded Peptides

Compound (Conformation)	log $P^{a)}$	pK_a	Total energy (kJ/mol)$^{b)}$
6a	5.639	11.7	−6907516.71
6b	5.639	11.7	−6907545.88
6c	5.639	11.7	−6907521.28
6e	4.895	11.7	−6315893.74
7a	6.418	—	−6514474.07
7b	6.418	—	−6514454.98
10	5.573	11.5	−4069383.15
Phenol	—	11.3 (9.89)$^{c)}$	—
Phe–Phe			
α-Helix like	1.797	—	−2695360.64
β-Sheet like	1.797	—	−2695353.11
Tyr–Phe			
α-Helix like	1.407	—	−2891870.70
β-Sheet like	1.407	—	−2891858.00

a) Ghose–Crippen method.[18] *b*) At HF/6-31G(d) level. *c*) The value in water. The Merck index, thirteenth edition (by Merck & CO. Inc.).

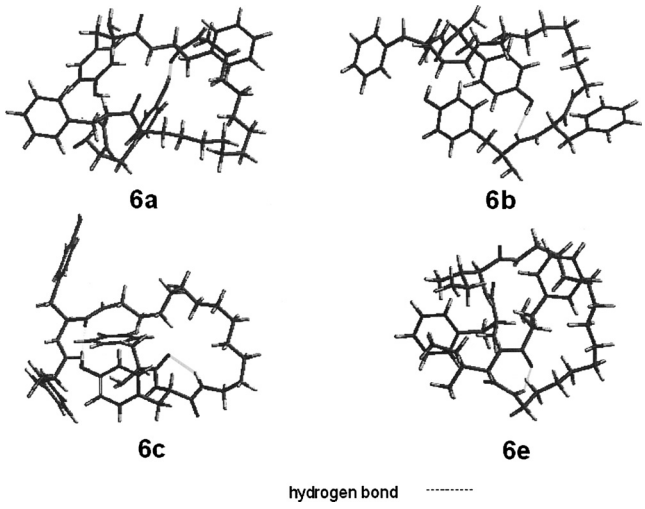

Fig. 2. Optimized Structures of Double-Stranded Peptides **6a**, **b**, **c**, and **e**

At *ab initio* HF/6-31G(d) level. The hydrogen bondings C=O···H–O–C_6H_4–CH_2– are observed in the intramolecules.

by spectrophotometric pH titration method from pH 4.96 to pH 12.55 in buffer (in 85% MeOH solution) to evaluate the behavior of phenolic protons. All UV/visible titration data were analyzed by plots of pH *versus* λ_{max} and showed a one-proton curve. In the plot generated for **6a**, two buffer regions were found as shown in Fig. 3B: one from pH 7.73 to pH 4.96 and another from pH 12.55 to pH 8.26. The initial deprotonation of **6a** gave a value for the logarithmic acid-base equilibrium constant (pK_a) of 11.7. This equilibrium is shown in Eq. 2. The equilibrium constant (11.7) of the phenolic protons of **6a** is lower than the value (11.3) of phenol

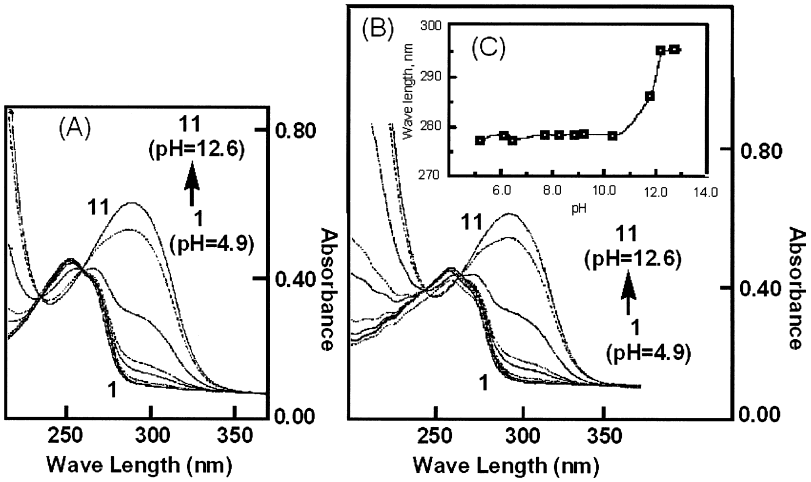

Fig. 3. Determination of the Acid-Base Equilibrium of Double-Stranded Peptides **6a** and **6e** Containing Tyr, Using the UV/Vis Titration Method

The determined acid-base equilibrium (pK_a) of **6e** (3.65×10^{-5} mol/l) (A) and **6a** (3.65×10^{-5} mol/l) (B) using 0.01 mol/l buffer (final concentration) prepared with 0.1 mol/l acetate, 0.1 mol/l sodium acetate, 0.2 mol/l borate-sodium chloride, and 0.2 mol/l sodium hydroxide buffer (85% MeOH). UV/vis spectra in range of pH 4.9, 6.1, 6.4, 7.7, 8.2, 8.8, 9.2, 10.4, 11.7, 12.2, and 12.6. (C) pH *vs.* λ_{max} curve for **6a**.

only. Single-stranded peptide (**10**)[4] however, showed a pK_a of 11.5, a lower value than double-stranded peptides **6a** or **6e**. The equilibrium shown in Eq. 2 shifts to the left side hand pass two protons dissociation since pK_a is small value.

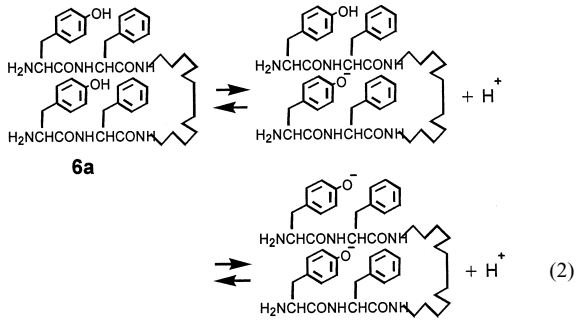

(2)

The decrease in the acidity suggests that the hydrophobic environment around the phenylalanine side chain and hydrophobic spacer of **6a** are changing, and that the local dielectric constant ($\Delta\varepsilon$) and log *P* increase more than Phenol because the pK_a value of peptide **10** is smaller than that of double-stranded peptide **6a**. We think that compound **6a** is folded, and that the two strands are interacting (Fig. 2).

Diasteromeric Effect on Anti-proliferative Activity of MCF-7, DU145, and A431 Cell Growth Table 2 and Fig. 4 show IC_{50} values of A431 and MCF-7 and DU145 cells treated with the double-stranded peptides **6a**, **b**, **c**, or **d** for 4 d. The peptides inhibited cell growth in the concentration range 10^{-4} to 10^{-6} mol/l. In A431 cell proliferation, compound **6a** was effective at concentrations greater than 331 μmol/l, while the diastereomer, bis(L-Tyr–D-Phe)-*N*,*N*-dodecane-1,12-diamine (**6b**), was more active (50.1 μmol/l) than **6a**. To further investigate the effect of the chilarity of the L- and D-configurations, we evaluated MCF-7 and DU145 cell growth inhibition following treatment with several synthesized double-stranded peptide analogs **6a**—**d**. Similar trends were found in MCF-7 and DU145 cells (Figs. 4A, B). Compound **6b**, with D-Phe, showed greater inhibition of MCF-7 and DC145 cell growth than **6a**. Compound **6c**, containing the reverse sequence to **6a**, –L-Tyr–L-Phe– was as effective as **6a**. Compound **6d**, containing the reverse sequence to **6b**, showed seven times less inhibition of MCF-7 cell proliferation than **6b**. However, compound **6d** is a more active inhibitor than **6a**, and **6d** is as active as the diastereomer **6b** on DU145 cell proliferation.

Table 2. Diastereomer-Specific Effect of Double-Stranded Peptides Contained Tyrosine Residue against Inhibition of A431 Cell Proliferation

Compound	Side chain[a)]		A431 cells IC_{50} ($\times10^{-6}$ mol/l), at 37 °C
	A	B	
6a	L-$CH_2C_6H_5$	L-$CH_2C_6H_4p$OH	>331.0
6b	D-$CH_2C_6H_5$	L-$CH_2C_6H_4p$OH	50.1
6e	L-$CH_2(CH_3)CH_2CH_3$	L-$CH_2C_6H_4p$OH	>331.0

a) The A and B represent the side chain of amino acid residues, Phe or Tyr.

These results suggest that the compounds **6b** and **6d** containing –L-Tyr–D-Phe– or –D-Phe–L-Tyr– sequence are able to inhibit malignant neoplastic proliferation.

Diasteromeric Effect on the Anti-proliferative Activity of *Src*^{ts}NRK Cells In order to further understand the relationship between the chirality of –x-Phe–x-Tyr– and anti-proliferative activity, compounds **6a**, **6b**, and **6e** were tested for anti-proliferative activity in *src*^{ts}NRK cells using a similar method as described above. The results are listed in Table 3. Anti-proliferative potencies of compounds **7a** and **7b**, containing –L-Phe–L-Phe– or –D-Phe–L-Phe– sequences, were also compared to those of **6a**, **6b**, and **6e**. To elucidate the mechanism of this inhibition, we compared the anti-proliferative potency of **6a**, **6b**, **7a** and **7b** with erbstatin (**8**) and genistein (**9**); both are inhibitors of tyrosine kinases.

Compound **6a** (IC_{50} >2000 μmol/l) had markedly less antiproliferative activity than the diastereomer **6b** containing D-Phe; it was found that compound **6b** was about 23 times more active than **6a** as an anti-proliferation agent of *src*^{ts}NRK cells transformed at 33 °C. The results showed the followed following order of potency against proliferation of *src*^{ts}NRK cells: **7b**>**6e**>**7a**>**8**>**9**>**6b**>**6a**, as shown in Figs. 5A and B. The mean anti-proliferative activities of **6b** and **6e** on the transformed *src*^{ts}NRK cells were found to

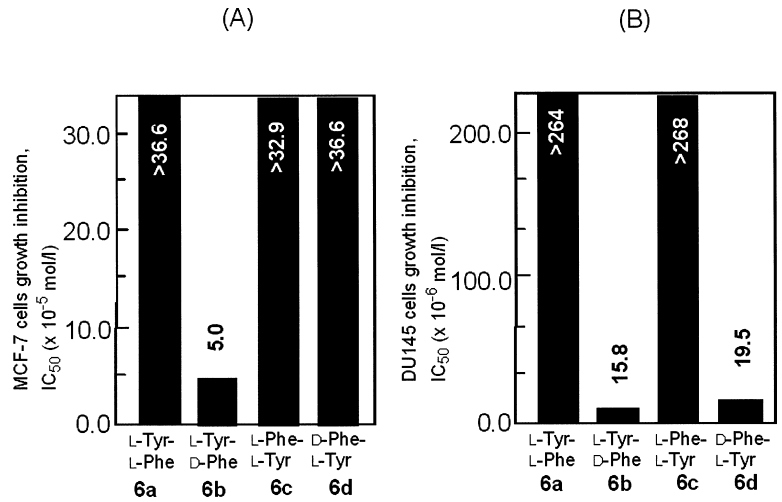

Fig. 4. Diasteromeric Effects of Double-Stranded Peptides (**6a**—**d**) Containing Tyr Residue on MCF-7 and DU145 Cell Proliferation

MCF-7 and DU145 cells were treated with double-stranded peptides (**6a**—**d**) or without peptides for 4 d. The IC_{50} was determined as described in Experimental. Each of the bars is the mean of two independent determinations at $<\pm 5\%$ of the absolute errors. (A) and (B) show IC_{50} values for MCF-7 and DU145 cells, respectively.

Table 3. Diastereomer-Specific Effects of Double-Stranded Peptides Contained Tyrosine Residue against Inhibition of *src*^{ts}NRK Cell Proliferation at 33 °C and 39 °C

Compound	Side chain[a]		*src*^{ts}NRK IC_{50} ($\times 10^{-6}$ mol/l)	
	A	B	33 °C	39 °C
6a	L-$CH_2C_6H_5$	L-$CH_2C_6H_4pOH$	>2140	>2140
6b	D-$CH_2C_6H_5$	L-$CH_2C_6H_4pOH$	88.0	205.0
6e	L-$CH(CH_3)C_2H_2CH_3$	L-$CH_2C_6H_4pOH$	16.1	30.1
7a	L-$CH_2C_6H_5$	L-$CH_2C_6H_5$	19.5	16.5
7b	L-$CH_2C_6H_5$	D-$CH_2C_6H_5$	2.3	5.7
8b	—	—	13.4	6.2
9	—	—	37.0	33.3

a) The A and B represent the side chain of amino acid residues, Phe or Tyr.

be 88.0 μmol/l and 16.1 μmol/l at 33 °C, respectively. The results showed that **6b** was about two times more active and **6e** was two times more active in normal *src*^{ts}NRK cells at 39 °C. Compounds **6b** and **7b**, containing D-Phe, have greater anti-proliferative activity against *src*^{ts}NRK cells with a transformed morphology than against those with a normal morphology. Compounds **8** and **9** potently inhibit normal *src*^{ts}NRK cell growth.

Why are double-stranded peptides **6b** and **7b** with –L-Tyr–D-Phe– and –D-Phe–L-Phe– sequences the most active? The observed difference in activity, particularly in the relatively high levels seen with double-stranded peptides **6b** and **7b** with –L-Tyr–D-Phe– and –D-Phe–L-Phe– sequences, may relate to their influences on cell death. The conjugation of D-Phe and L-Tyr to the chemicals may enhance their anti-proliferative activity.

Western Analysis of Phospho-Tyrosine in *Src*^{ts}NRK Cells To elucidate the mechanism of the inhibition of cell proliferation, we examined the changes in the tyrosine phosphorylation of proteins. *Src*^{ts}NRK cells were cultured in the presence of non-active concentrations of double-stranded peptides, **7a**, **7b**, **6a**, or **6e**, for 24 h at 33 °C and the lysates were extracted from the cells. The cells (1×10^8 cells/ml) were homogenized in 2 ml of lysis buffer, using a homogenizer. The lysates were analyzed by Western blotting using anti-phosphotyrosine antibody (peroxidase-labeled PY20),[19] as shown in Fig. 6B. Figure 6A presents the SDS-PAGE gel

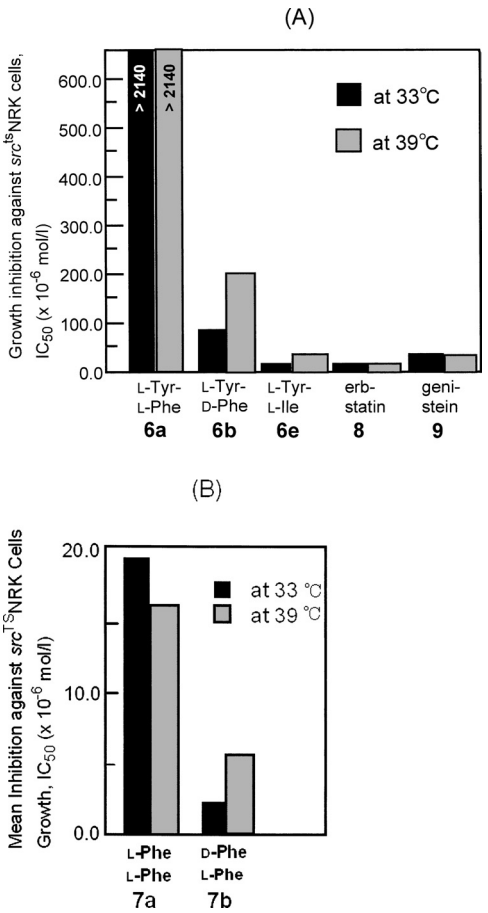

Fig. 5. Diastereomeric Effects of Double-Stranded Peptides Conjugated with Tyrosine on *Src*^{ts}NRK Cell Proliferation

Src^{ts}NRK cells were treated with or without double-stranded peptides **6a**, **6b**, and **6e**, and tyrosine kinase inhibitors, erbstatin (**8**) and genistein (**9**), for 4 d at 33 °C and at 39 °C, respectively. IC_{50} values were determined as described in Experimental. Each of the bars is the mean of two independent determinations at $<\pm 5\%$ of the absolute errors.

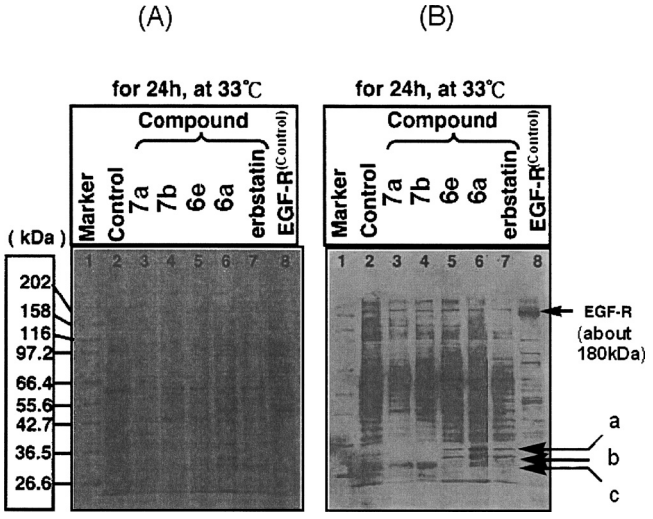

Fig. 6. Structure-Dependent Selective Effects of Double-Stranded Peptides Conjugated with Phe and Tyr on tyrosine Phosphorylation of Proteins in *Src*^{ts}NRK Cells

Src^{ts}NRK cells were incubated without (control) and with **7a** (1.3×10^{-5} mol/l), **7b** (1.9×10^{-6} mol/l), **6e** (1.1×10^{-5} mol/l), **6a** (1.1×10^{-5} mol/l), and **8** (8.8×10^{-6} mol/l) for 24 h at 33 °C. Total proteins were extracted from the cells as described in Experimental and analyzed by 8% SDS-PAGE gel electrophoresis (A). Subsequently, phosphotyrosine-containing proteins were detected by Western blotting (B). Lane 8 is the EGF receptor.

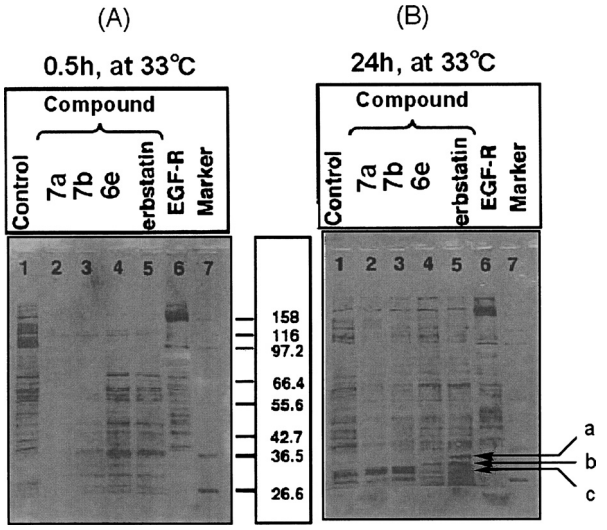

Fig. 7. Time-Course of Protein Phosphorylation in *Src*^{ts}NRK Cells Treated with Double-Stranded Peptides Conjugated with Phenylalanine and Tyrosine

Src^{ts}NRK cells were incubated without (control, lane 1) and with (experimental, lanes 2, 3, 4, and 5) **7a** (1.3×10^{-5} mol/l), **7b** (1.9×10^{-6} mol/l), **6e** (1.1×10^{-5} mol/l), and erbstatin **8b** (8.8×10^{-6} mol/l) for 0.5 (A) and 24 h (B), respectively. The cells were then extracted and phosphotyrosine-containing proteins were analyzed by Western blotting as described in Experimental. Lane 6 is the EGF receptor.

profile of the cell lysates cultured without double-stranded peptides, stained with CBB dye.

Compounds **7a** and **7b** show heterogeneous gel profiles of tyrosine phosphorylation of total proteins when compared to the control (Fig. 6A and lane 2 in Fig. 6B). Compounds **7a** and **7b** induced the tyrosine phosphorylation of approximately 30 kDa proteins (c at lanes 3 and 4 in Fig. 6B) since the proteins disappear in the results with CBB staining (lanes 3 and 4 in Fig. 6A). However, compounds **6a** and **6e** induced the tyrosine phosphorylation of approximately 33 and 35 kDa proteins (a and b at lanes 5 and 6 in Fig. 6B) but not of approximately 30 kDa proteins (c at lane 5 in Fig. 6B). The results of tyrosine phosphorylation following treatment with **6a** and **6e** were compared with the results of tyrosine phosphorylation following treatment with erbstatin. Interestingly, the results of **6a** and **6e** showed similar gel profiles to those of tyrosine phosphorylation following treatment with erbstatin (lane 7 in Fig. 6B). The gel mobility of the bands of a and b in (lane 7 in Fig. 6B) are consistent with tyrosine phosphorylation by erbstatin.

In addition, the tyrosine phosphorylation of EGF-R, a receptor-type protein tyrosine kinase, following treatment of *src*^{ts}NRK cells with peptide **6a** was observed at a molecular weight of about 180 kDa (lane 6 in Fig. 6B). The tyrosine phosphorylation of EGF-R following treatment with **7a**, **7b**, **6e**, and erbstatin was also observed in other lanes (lanes 3, 4, 5, and 7 in Fig. 6B). These results indicate that compounds **6a** and **6e**, with conjugated Tyr residues, inhibit the action of tyrosine kinase.

Time Course of Phosphorylation in *Src*^{ts}NRK Cells We examined the time course of tyrosine phosphorylation following treatment with **7a**, **7b**, **6e**, and erbstatin analog (**8b**) in *src*^{ts}NRK cells. The results are shown in Fig. 7. *Src*^{ts}NRK cells were cultured with 0.5% FBS/DMEM medium for 24 h and with 10% FBS/DMEM medium in the presence of **7a** (1.3×10^{-5} mol/l), **7b** (1.9×10^{-6} mol/l), **6e** (1.1×10^{-5} mol/l), and **8b** (8.8×10^{-6} mol/l) at 33 °C for 0.5 and 24 h, respectively. The pattern of total tyrosine phosphorylation obtained with **6e** was strikingly similar to those obtained with **8b** at 0.5 and 24 h (lanes 4 and 5 in Figs. 7A and B). The pattern is different from that of **7a**, **7b** or control (Fig. 7). Moreover, it found that compounds **7a** or **7b** conjugated –Phe–Phe– inhibit total protein tyrosine phosphorylation at least 0.5 h (lanes 2 and 3 in Fig. 7A). At 24 h, the patterns of the total protein tyrosine phosphorylation obtained with **6e** differed from those obtained with **7a** or **7b** (Fig. 7B). Compound **7a** or **7b** stimulation of *src*^{ts}NRK cells resulted in tyrosine phosphorylation of proteins with 30 kDa (arrow a in lanes 2 and 3 in Fig. 7B) which is different from tyrosine phosphorylated 33 kDa and 35 kDa proteins (arrows a and b in lanes 4 and 5 in Fig. 7B) obtained with **6e** or **8b**. From lanes 4 and 5 in Fig. 7B, it appears that treatment with **6e** (or **6a**) increases the levels of tyrosine phosphorylated 33 kDa and 35 kDa proteins. In addition, the levels of the protein tyrosine phosphorylated EGF-R (180 kDa) by treatment with **7a**, **7b**, **6e**, and **8b** are higher than the control level (Fig. 7B). Although compounds **7a** and **7b** are more potent inhibitors than **6e** in *src*^{ts}NRK cells, the pattern of total tyrosine phosphorylation differs from that of the erbstatin analog. Compound **6e** is similar to the pattern of the total protein tyrosine phosphorylation of proteins with **8b** in *src*^{ts}NRK cells. Compound **6e** (or **6a** and **b**, *etc.*) may have similar mechanisms compared with **8b**.

Effects of Double-Stranded Peptides on Tyrosine Phosphorylation Activity of EGFRKD The inhibition of protein tyrosine phosphorylation by this series of double-stranded peptides was tested with epidermal growth factor receptor (EGFR) activation of tyrosine protein kinase activity. Relative levels of EGFRKD autophosphorylation follow-

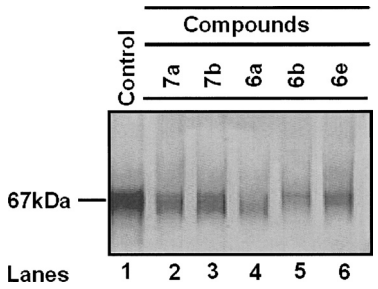

Fig. 8. Effects of Double-Stranded Peptide Conjugated with Phenylalanine and Tyrosine **6a**, **6b**, **6e**, **7a**, and **7b** on Autophosphorylation of EGFRKD

EGFRKD was treated with the indicated concentrations of compounds **6a**, **6b**, **6e**, **7a**, and **7b**, (lanes 2—6) for 10 min at 22 °C. The levels of autophosphorylation of EGFRKD were visualized by Western blotting using HRP labeled anti-phosphotyrosine antibodies as described in Experimental. Lane 1 is the control.

ing inhibition by double-stranded peptides were analyzed by Western blotting using anti-phosphotyrosine antibodies (peroxidase-labeled PY20),[19] as shown in Fig. 8. Lane 1 (control) shows the result of autophosphorylation of EGFRKD without double-stranded peptides. As shown in lanes 2 to 6, the level of autophosphorylation of EGFRKD after treatment with double-stranded peptides decreases in comparison with the level of autophosphorylation in the control. However, we found that the level of the autophosphorylation of EGFRKD treated with compounds **6a**, **6b**, or **6e** (lanes 4—6 in Fig. 8) is lower than the level of autophosphorylation of EGFRKD treated with the compounds **7a** or **7b** (lanes 2 to 3 in Fig. 8). The results showed that the autophosphorylation of EGFRKD is inhibited by compounds **6a**, **6b**, and **6e**, conjugated with Tyr. We showed, especially, that **6a** and **6b**, containing D-Phe and L-Tyr residues, inhibit the autophosphorylation of EGFRKD more than **6e**, **7a** and **7b**. Therefore, the action of **6a** and **6b** may act similar to products such as gefitinib (Iressa™),[10] to inhibit the growth of EGFR-positive cancer cell lines with or without erbB2 overexpression (Fig. 8).

Conclusions

The double-stranded peptides **6a**, **6b** and **6e**, conjugated with Tyr, have a different mechanism than **7a** and **7b**, conjugated only with Phe, in the inhibition of cell proliferation. Anti-proliferative activity of **6a**, containing Tyr, is lower than **7a**. Moreover, we found that the diastereomer **6b** is more active than **6a**. Although **6a** and **6b** affect protein tyrosine phosphorylation of approximately 30, 33, and 35 kDa proteins in *src*^{ts}NRK cells, **7a** and **7b** did not affect the phosphorylation of these proteins. We found that the action of **6a** and **6b** is similar to that of erbstatin, a protein tyrosine kinase inhibitor, from the results of tyrosine phosphorylation using anti-phosphotyrosine antibody. To elucidate the effect on protein tyrosine phosphorylation of **6a** or **6b**, we investigated the action of EGFRKD following treatment with the compounds. As **6a** and **6b** reduce the level of EGFRKD autophosphorylation, they probably inhibit the action of EGF-R and other protein tyrosine kinases in cells. In addition, the diastereomers **6b** and **7b** inhibit the growth of DU145, MCF-7, and *src*^{ts}NRK cells more actively than **6a**, **6c** and **7a**. These results indicate that diastereomers **6b**, **6d** and **6e** have bioactive conformations and side chains and are key compounds for the development of new drugs to treat cancer and other diseases.

Acknowledgments We would like to thank Dr. Hideki Suzuki, Ms. Tamiko Kiyotani, and Mr. Youichi Takase for NMR and FAB-MS measurements (Showa Pharmaceutical University, Tokyo).

References and Notes

1) Ullrich A., Schlessinger J., *Cell*, **60**, 203—212 (1990).
2) Aaronson S. A., *Science*, **254**, 1146—1152 (1991).
3) Koch C. A., Anderson D., Moran H. F., Ellis C., Pawon T., *Science*, **252**, 668—674 (1991).
4) Kobayashi S., Kobayashi H., Yamaguchi T., Nishida M., Yamaguchi K., Kurihara M., Miyata N., Tanaka A., *Chem. Pharm. Bull.*, **48**, 920—934 (2000).
5) Kobayashi S., Atuchi N., Kobayashi H., Shiraishi A., Hamashima H., Tanaka A., *Chem. Pharm. Bull.*, **52**, 204—213 (2004).
6) Kobayashi S., Wakamatsu H., Atuchi N., Miyajima R., Kawada A., Hattori M., *Chem. Pharm. Bull.*, **55**, 7—14 (2007).
7) Downward J., Parker P., Waterfield M. D., *Nature* (London), **311**, 483—485 (1984).
8) Traxler P., Trinka U., Buchdunger E., Mett H., Meyer T., Muller M., Regenass U., Rosel J., Lydon N., *J. Med. Chem.*, **38**, 2441—2448 (1995).
9) Umezawa K., Tanaka K., Hori T., Abe S., Sekizawa R., Imoto M., *FEBS Lett.*, **279**, 132—136 (1991).
10) Anderson N. G., Ahmad T., Chan K., Dobson R., Bundred N. J., *Int. J. Cancer*, **94**, 774—782 (2001).
11) Spartan 04 is a molecular orbital software package (Wavefunction, Inc., Irvine, CA).
12) Fabricant R. N., DeLarco J. E., Todaro G. J., *Proc. Natl. Acad. Sci. U.S.A.*, **74**, 565—569 (1977).
13) Liber M., Smith B., Szakal A., *Int. J. Cancer*, **17**, 62—70 (1976).
14) Suzukake-Tsuchiya K., Moriya Y., Kawai H., Hori M., Uehara Y., Iinuma H., Naganawa H., Takeuchi T., *J. Antibiot.*, **44**, 344—348 (1991).
15) Uehara Y., Hori M., Takeuchi T., Umezawa H., *Jpn. J. Cancer Res.*, **76**, 672—675 (1985).
16) Kobayashi S., Shinohara H., Tabata K., Yamamoto N., Miyai A., *Chem. Pharm. Bull.*, **54**, 1633—1638 (2006).
17) Delepierre M., Dobson C. M., Poulsen F. M., *Biochemistry*, **21**, 4756—4761 (1982).
18) Ghose A. K., Pritchett A., Crippen G. M., *J. Comput. Chem.*, **9**, 80—90 (1988).
19) Glenney J. R., Zokas L., Kamps M. J., *J. Immunol. Methods*, **109**, 277—285 (1988).